Grant Agreement No 727689

Document Title:
Novel Materials for Blade Design

Document No:
RLT-WP5-2-PDL-001-00

Status Code	Description
A	Accepted
B	Issued for Acceptance
C	Issued for Review
D	Information Only Approval not required
E	Cancelled

00	B	/	Mael Arhant, Peter Davies (IFREMER) Joseph Praful Tomy (BV) 25/11/2020	All partners 25/11/2020	Stephane Paboeuf (BV) 30/11/2020
Rev No	Status	Revision Description	Prepared By / Date	Reviewed By / Date	Approved By / Date

European Commission
H2020 Programme for Research & Innovation

Advanced monitoring, simulation and control of tidal devices in unsteady, highly turbulent realistic tide environments

REALTIDE

Grant Agreement number: 727689

Project Acronym: RealTide

Project Title: Advanced monitoring, simulation and control of tidal devices in unsteady, highly turbulent realistic tide environments

Deliverable D5.2
Novel Materials for Blade Design

WP 5
Novel and Advanced Components

WP Leader:
Sabella SAS

Dissemination level:
Public

Summary:
This document presents results from an investigation performed at IFREMER to evaluate the durability of alternative composite materials for tidal turbine blades. The report consists of two parts; the first examines the mechanical properties of four novel composite combinations (carbon/PA6, carbon/green epoxy, glass/PP and flax/acrylic) and compares them to those of traditional carbon and glass/epoxy composites. The second part examines the influence of seawater immersion on properties under quasi-static and cyclic loading.

Objectives:
The aim if this study is to determine to what extent materials with reduced environmental impact can be employed as alternatives to fibre reinforced petrochemical based resins in tidal turbines. One option studied is the use of thermoplastic matrix resins, which can be recycled to some extent at the end of the turbine service life. The second option is to investigate whether natural fibres, flax here, can replace glass fibres in a blade design. This report provides the data for this evaluation, the analysis of the impact of these materials on blade design will be performed in WP 5.1.

Table of Contents

List of Figures

List of Tables

1 INTRODUCTION

This report presents the results from a study performed to evaluate alternative blade materials with reduced environmental impact, as part of the EU H2020 RealTide project (WP 5.2).

2 BACKGROUND

Whereas carbon fibre reinforced epoxy composite is the most widely used material for tidal turbine blade manufacture today, there are a number of alternative materials which offer potential for lower costs and/or lower environmental impact. The use of bio-sourced materials for composite construction has been of increased interest in the recent times. A comprehensive list of advantages and disadvantages of such fully green composites is extracted from [1], and shown in Figure 1.

Advantages	Disadvantages
Less expensive	Lower mechanical properties (especially impact strength)
Lower weight	Higher moisture absorption
Higher flexibility	Lower durability
Renewable	Poor fire resistance
Biodegradable	Variation in quality
Good thermal and sound insulation	Restricted maximum processing temperature
Eco-friendly	Poor microbial resistance
Nontoxic	Low thermal resistance
Lower energy consumption	Demand and supply cycles
No residues when incinerated	
No skin irritations	

Figure 1: Summary of advantages and disadvantages of fully green composites over traditional petrochemical-based composites

However, many of the “green” composite solutions proposed today do not provide the advantages shown in this table. For example, natural fibre reinforcements tend to be more expensive than traditional glass fibres, and bio-sourced matrix polymers are not necessarily biodegradable in a marine environment. As a result great care is needed when proposing alternative materials.

2.1 ALTERNATIVE MATERIALS

Composites are manufactured materials, whose properties can be tuned based on the type of resin and the type of fibres used for reinforcement. When speaking about alternative materials that can reduce the environmental impact, the selection of either the resin or the fibre can contribute towards such sustainability. The subsequent paragraphs discuss the various material options available from existing literature.

2.1.1 Alterative matrix polymers

In order to maintain their structural integrity at higher temperatures, thermoset resins are typically used in composite applications. Whereas the material strengthens on heating, it cannot be remolded or reheated after the initial forming. This presents a problem at the end of service life as the initial polymer cannot be recovered by any physical or chemical means. One alternative solution is the use of thermoplastics, which can be re-moulded by heating. Some examples of thermoplastics are

polypropylene (PP), polyethylene (PE), polyvinylchloride (PVC), polystyrene (PS), polyamide (PA), acrylic, polycarbonate, etc.
A classification of alternative matrix polymers, based on their degradability, is shown in Figure 2 [1]. However, the heading "fully degradable" indicates that there is potential to degrade the polymer completely but this does not necessarily occur under all conditions.

Another possibility for alternative polymers is to improve the reusability of thermoset polymers. A novel concept related to this has been presented in [2]. The approach is based on the introduction of reversible or exchangeable bonds into the polymer network. The concept is named 3R Composite – with enhanced re-processability, reparability and recyclability compared to typical thermoset polymers.

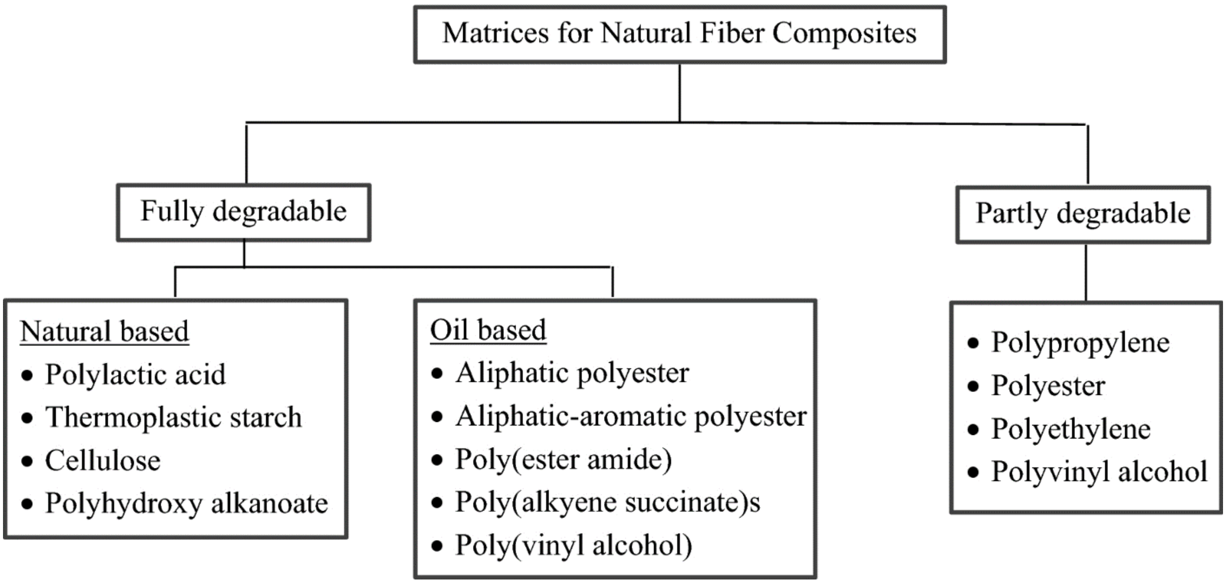

Figure 2: Classification of polymer matrices for natural fibre composites [1]

2.1.2 Alternative fibres

Replacing classical fibre materials such as glass and carbon with bio-sourced materials may present another means of improving the sustainability of composite manufacturing. Typical examples of bio-sourced fibres are wood, cotton, flax, kenaf and hemp. A classification of various natural fibres is shown in Figure 3. These materials are readily available, and less harmful to the environment. Other naturally occurring materials with significant mechanical properties, such as basalt, may also provide alternatives as eco-friendly reinforcements.

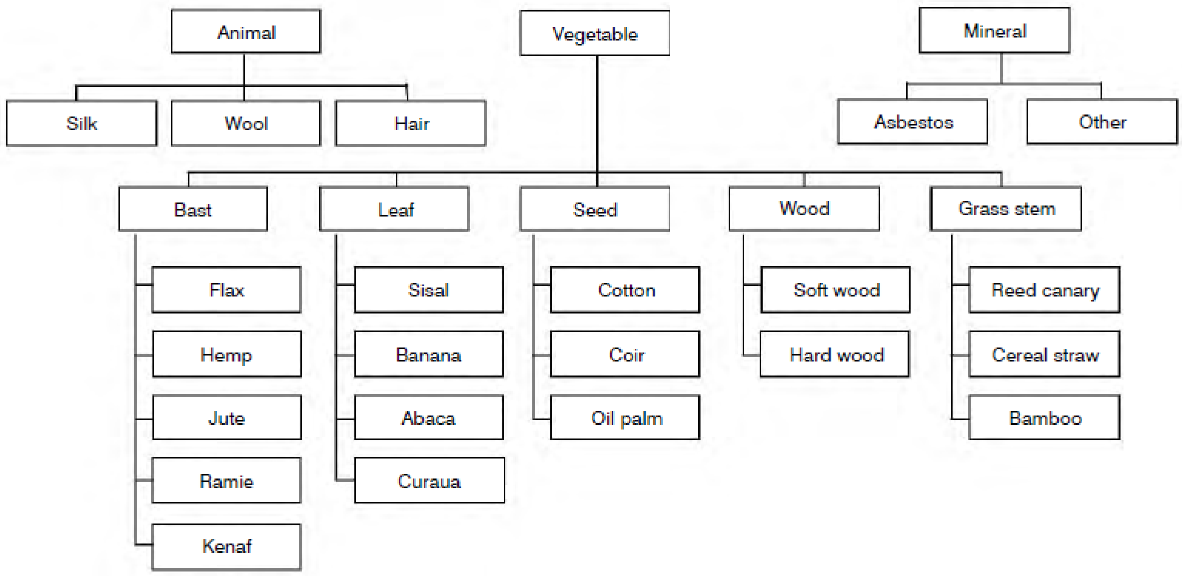

Figure 3: Types of natural fibres [3]

Natural fibre composites (NFCs) have a strength-weight ratio (or specific stiffness) comparable to glass fibre composites [4]. One perceived difficulty in using them for structural applications is the dispersion in the measured strength properties. A lack of reliability of the mechanical properties might make them not well-suited for the structural design, review and classification procedures generally followed for structural applications but this does not appear to be limiting the growing number of applications.

Hybrid composites are composites which have a combination of two or more reinforcement fibres. They are typically used when a combination of different properties are desired, such as better strength-weight ratio. The most common hybrid composites are (i) carbon-aramid reinforced epoxy, which combines strength and impact resistance, and (ii) glass-carbon reinforced epoxy, which gives a strong material at a reasonable price. Research on mechanical and chemical properties of various hybrid composites is ongoing. Some examples can be found for Kevlar reinforcement in kenaf composites [5] and sisal/carbon reinforced composites [6], which combine natural fibres with synthetic fibres. The potential applications of hybrid composites in aerospace applications have been explained by Jamir et al [7].

2.1.3 Alternative core material

As opposed to monolithic composite construction, sandwich core construction makes use of a core material in the middle of the laminate stacking sequence. The core may not act as a structural member, its main purpose is to increase the inertia of the laminate without the need for adding additional plies. For composite blade construction, the use of eco-friendly core materials can reduce the environmental impact. One such material that has been used in the marine field for many years is balsa wood. In addition to being eco-friendly, balsa wood is an excellent core material due to its good strength and stiffness properties. Cork can also be used as a core material.

2.2 MATERIAL PROPERTIES

The main driving factors behind the quest for alternate materials for tidal blade construction are the potential reduction in costs and/or environmental impact. At the same time, the mechanical properties of these materials have to be validated against those for the conventional materials used for tidal blade construction, such as carbon/epoxy or glass/epoxy composites. The main mechanical properties of interest are – Stiffness, Strength, Fatigue resistance, Impact damage tolerance and Seawater ageing resistance. In addition, relevant non-mechanical properties include cost and ease of manufacturing. The focus of the work performed under Task 5.2 of the RealTide project is to identify potential alternative materials for tidal blade construction, and to experimentally characterize the mechanical properties of such materials in comparison with conventional materials.

As mentioned earlier, the reliability of material properties of natural fibre composites is one of the key factors that count against it. Even though certain natural fibre materials such as flax have shown comparable mechanical properties to E-glass, when composite materials are manufactured from both fibres, the flax composite strengths are often lower than those of E-glass composites [8]. The variability of the mechanical properties of flax fibre composites has also been highlighted in the work of Baley et al [9]. Similar variability is expected for all agro-based fibres, where the mechanical properties depend on the method of cultivation, and processes for mechanical extraction and manufacture of fibres.

Environmental impact is not a criterion today, as most tidal turbines are at the prototype stage, but successful commercial development and a multiplication of the number of blades will lead to the question of life cycle analysis. It is important both to examine end-of-life options and to ensure that the benefits of cleaner energy are not offset by increased environmental impact.

3 MATERIALS SELECTED FOR THE STUDY

Based on an analysis of literature data and material availability it was decided to examine four alternative materials to the carbon and E-glass fibre reinforced epoxy materials characterized previously in WP 1.3:

- **Carbon fibre reinforced Green Epoxy™**. The epoxy resin produced by Sicomin SA is partially biobased.

- **Carbon fibre reinforced polyamide 6**. This thermoplastic matrix composite offers the possibility for recycling, and will allow a direct comparison with the carbon/epoxy composite used today for the Sabella (and most other) tidal turbine blades, characterized in WP 1.3.

- **Glass fibre reinforced polypropylene**. This material is also recyclable, polypropylene is an inexpensive thermoplastic with low sensitivity to moisture. Glass fibre composites have not received much attention for tidal turbine blades compared to carbon fibre composites but they should be cheaper, and glass/PP can be directly compared to the glass/epoxy characterized in WP 1.3.

- **Flax fibre reinforced acrylic**. This is a radically different option, involving a new potentially recyclable polymer matrix (Elium™ from Arkema), reinforced by natural flax fibres. It will allow a further comparison with the glass/epoxy characterized in WP 1.3.

Table 1 summarizes the different material systems investigated within this task, together with their environmental impacts and associated costs.

Table 1: Materials environmental impact and associated cost

Material	Fibre	Resin	Cost	Biobased Petrobased	Recyclable Repairable
1	Carbon	Polyamide 6	Similar cost	Petrobased	Yes
2	Glass	Polypropylene	Lower	Petrobased	Yes
3	Flax	Elium™	Lower	Partially biobased	Probably
4	Carbon	Green Epoxy	Similar cost	Partially biobased	No

4 MANUFACTURE

The selection of alternative materials can require a change in manufacturing procedures. The carbon/PA6 and glass/PP were manufactured by thermo-compression in a heated press. However, the flax/acrylic and carbon/green epoxy panels were manufactured using the same infusion process as the epoxy composites. Figure 4.a and Figure 4.b show the manufacturing cycles used for the C/PA6 and G/PP composites, respectively.

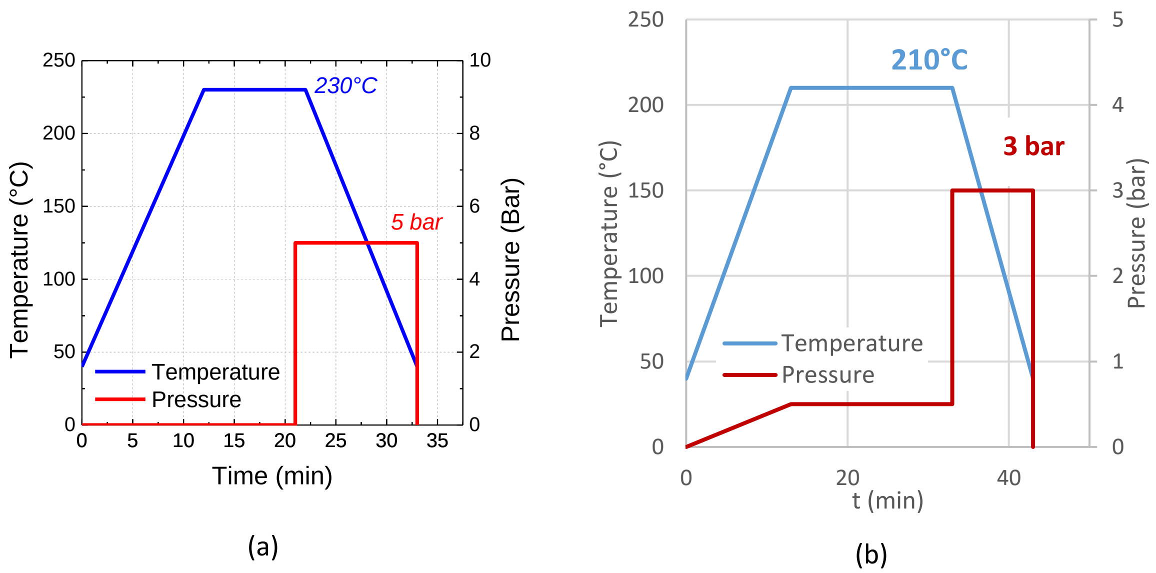

Figure 4: Manufacturing cycles for thermoplastic composites (a) Carbon/Polyamide 6 (b) Glass/Polypropylene

5 QUALITY CONTROL

5.1 RESULTS FROM THICKNESS MEASUREMENTS, DESNITY, FIBRE VOLUME FRACTION, AND RESULTS FROM DSC TESTS (MELT TEMPERATURE, DEGREE OF CRISTALLINITY)

Table 2 describes the four materials tested.

Table 2: Results from quality control

Material	Sequence	Thickness (mm)	Density (g/cm^3)	V_f (%)	T_g (°C)	T_m (°C)	X_c (%)
Carbon/PA6	$[0]_{8s}$	2.1 ± 0.1	1.13 ± 0.01	48 ± 1	66 ± 1	220	38
	$[\pm45]_{4s}$	2.1 ± 0.1					
	$[0_4/90_4]_s$	2.0 ± 0.1					
Glass/PP	$[0]_{2s}$	1.7 ± 0.1	1.67 ± 0.07	46 ± 1	-7	162	39
	$[\pm45]_{2s}$	2.0 ± 0.1					
	$[0/90]_s$	2.0 ± 0.1					
Flax/Elium	$[0]_s$	4.5 ± 0.1	1.18 ± 0.02	25*	56	/	/
	$[\pm45]_{4s}$	4.3 ± 0.1			64		
	$[0/90]_s$	4.6 ± 0.2			64		
Carbon/GreenPoxy33	$[0]_{2s}$	2.3 ± 0.1	1.40 ± 0.03	60 ± 1	81	/	/
	$[\pm45]_s$	2.0 ± 0.1	1.55 ± 0.01	57 ± 1	69		
	$[0/90]_s$	2.4 ± 0.1	1.46 ±0.01	62 ± 1	81		

5.2 ULTRASONIC C-SCANS

To check the overall quality of the different panels, ultrasonic C-scans were performed. Results for the C/PA6, G/PP and F/El are respectively shown in Figure 5.a, Figure 5.b and Figure 5.c. From experience, attenuations higher than 16 dB usually correspond to macrovoids found within the panels. First, these results suggest that the Flax/Elium panel is of a lower quality compared with the C/PA6 and G/PP panels. However, the microstructure of flax fibres is very different compared to the carbon and glass counterparts, so these can hardly be compared directly. More especially flax fibres possess a hollow core which other fibres like carbon and glass do not. Second, the other two panels show low levels of attenuation, typically below 10 dB. The edges of the G/PP panels display much higher levels of attenuation (>16dB), so samples were not taken from these particular areas.

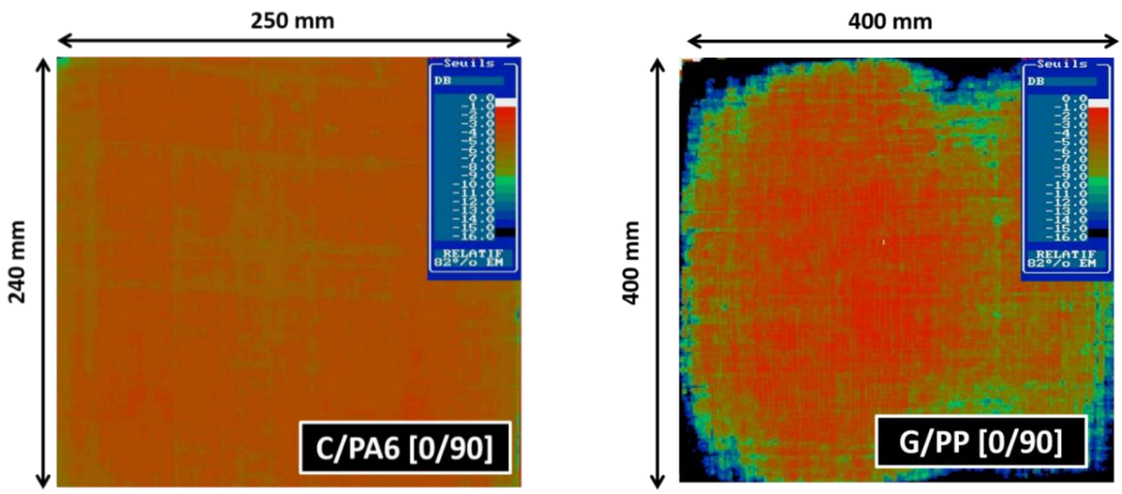

(a) (b)

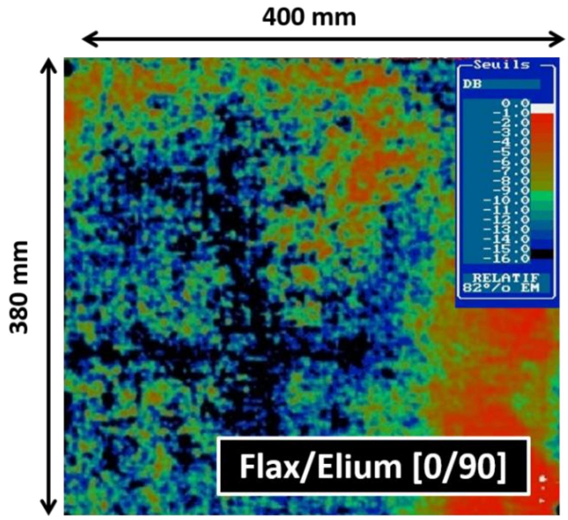

(c)

Figure 5: Ultrasonic C-scans on [0/90] panels using an attenuation scale of 16dB (a) Carbon/Polyamide (b) Glass/Polypropylene (c) Flax/Elium

Then, results concerning the [0] and [±45] C/GR33 panels are shown in Figure 6.a and Figure 6.b, respectively. Results show that the [±45] panel is of an excellent quality as attenuation levels observed here are all below 4 dB. Then, the unidirectional panel is of a lesser quality compared to the [±45] panel. To confirm this, optical microscopy was carried out. Results are presented in the next section.

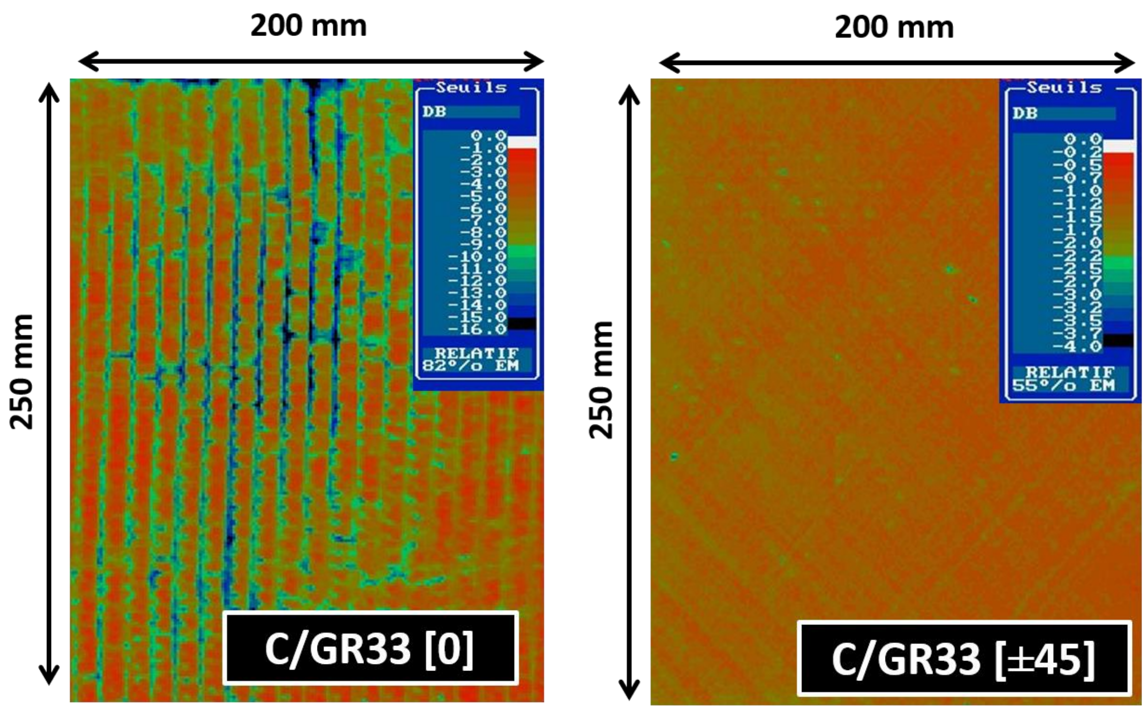

(a) (b)

Figure 6: Ultrasonic C-scans on the Carbon/GreenPoxy 33 panels (a) [0] Attenuation scale = 16 dB (b) [±45] Attenuation scale = 4 dB

5.3 OPTICAL MICROSCOPY

Polished sections for C/PA6, G/PP and F/El are respectively shown in Figure 7.a, b and c. Concerning the first two, results from optical microscopy show very low void contents. A few microvoids are observed for the G/PP panel and no voids are clearly seen in the C/PA6 panel. This agrees with results from ultrasonic C-scans in Figure 5 (the section of G/PP was extracted from the centre of the panel). For the F/Elium™ material, the polished section cannot be used to draw a direct conclusion despite the fact that a few dark spots are observed.

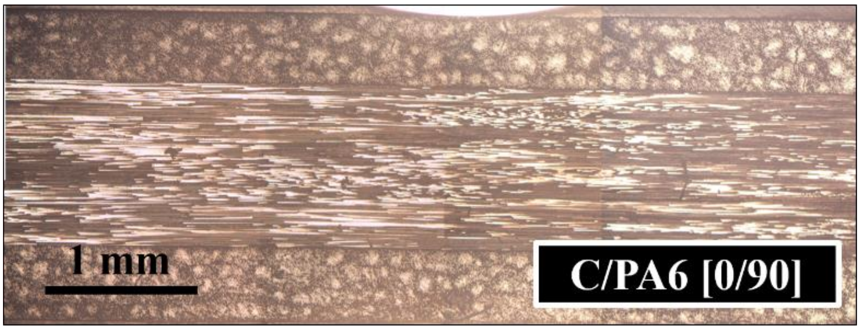

(a)

(b)

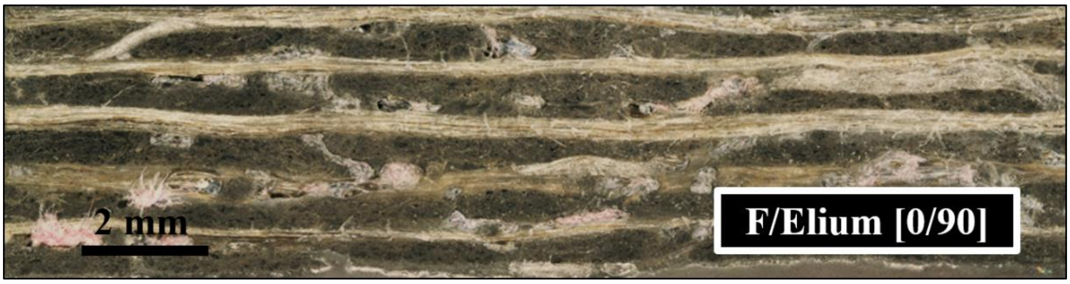

(c)

Figure 7: Polished sections for specimens extracted from (a) C/PA6 (b) G/PP (c) F/El panels

Then, polished sections concerning the unidirectional and biaxial panels from the C/GR33 material are respectively shown in Figure 8.a and b.

Again, results are in close agreement with those of ultrasonic C-scans in Figure 6. Micro and macro voids are observed in the unidirectional panel while very few microvoids are observed for the biaxial panel.

(a)

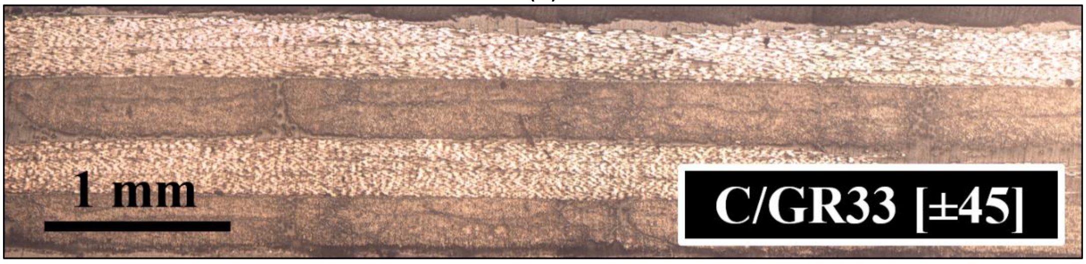

(b)

Figure 8: Polished sections for specimens extracted from the C/GR33 panels (a) [0] (b) [±45]

6 SEA WATER AGING

The water absorption was determined from the weight evolution of square samples at 40°C on the flax/elium, carbon/polyamide 6 and glass/polypropylene laminates. Sea water aging was not carried out on the carbon/greenpoxy33 laminates because these materials were received too late, shortly before the end of the T5.2 activity, due to the pandemic situation.

The different samples were immersed in natural renewed sea water from Brest estuary. The mass gain was followed by periodic weighing of the different specimens on a Sartorius LA310 S balance having a precision of 0.1 mg. Before each measurement in immersion, the water on the surface of the specimen was wiped off with a paper towel. For each measurement, three samples were used at each time. The water content, M(t) in wt.% of a sample is defined as follows, Eq. 1.

$$M(t) = \frac{m(t) - m_0}{m_0} \times 100 \qquad \text{Eq.1}$$

Where m(t) is the mass of the sample at a time t and m_0 the initial mass of the sample. The sea water aging tanks are shown in Figure 9.

Figure 9: Sea water aging tanks at Ifremer in Brest

Results from sea water absorption tests are shown in Figure 10. These specimens were immersed for durations up to 3 months in sea water.

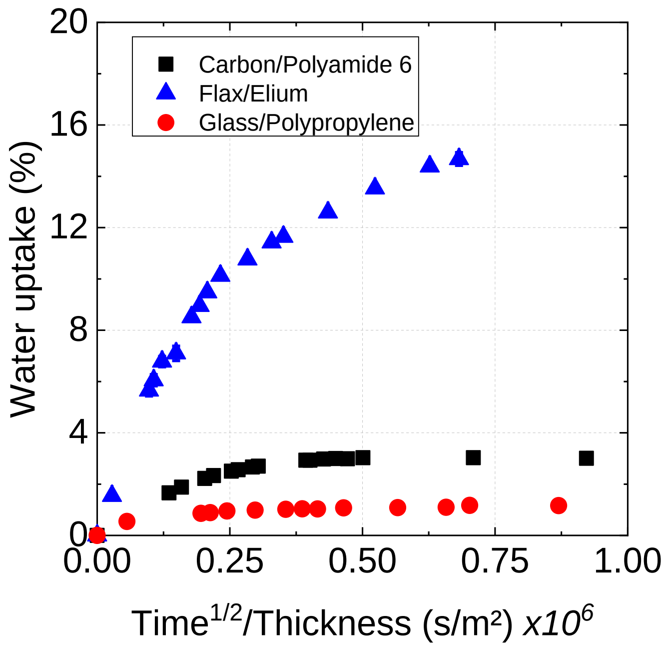

Figure 10: Sea water absorption during immersion at 40°C

Results from Figure 10 show that the three materials investigated here behave very differently when immersed in sea water. The Flax/Elium™ laminate absorbs a significant amount of water (M_{sat}>15%) at a much faster rate than the other two materials. This may be associated with the fact that both the flax fibres and the matrix absorb water, while the carbon and glass fibres do not. The Carbon/Polyamide 6 materials absorbs around 3% percent of water at saturation and the glass/polypropylene laminate absorbs around 1% of water. The water contents at saturation are shown in Table 3 for the three materials although the flax composite weight is still increasing slowly.

Table 3: Water contents at saturation at 40°C

Material	Water content at saturation (%)
Carbon/Polyamide 6	3.01 ± 0.01
Glass/Polypropylene	1.16 ± 0.06
Flax/Elium	16 ± 3

7 QUASI-STATIC PROPERTIES

The quasi static properties of all four materials are characterized in this section. First, these were determined in tension, then in flexure. For all these tests, five repeat specimens were used. All results presented within the tables in the following sections correspond to average values ± standard deviation.

7.1 TENSILE TESTS

7.1.1 Tests on unidirectional specimens in the longitudinal direction [0]

First tensile tests were performed on unidirectional specimens along the longitudinal direction in order to obtain the elastic modulus E_1, the poisson's ratio ν_{12} and the longitudinal strength σ_1. Results are summarized in Table 4and figures are found in the appendix at the end of this document. The rule of mixtures, Eq. 2, was used to verify whether the properties obtained within this experimental campaign are in agreement with the theory. Data for the calculation were taken from literature and are found in

Table 5.

Experimental results are very close to those from the theory. However, the rule of mixtures always leads to higher values than those from experimental tests, which may be associated with the fact that process, and so void content is not considered in the calculation. Concerning this, it was noted earlier that it is quite difficult to measure with accuracy the fibre volume content of flax reinforced composites. Here, the value (V_f) was adjusted in order to fit with experimental data. Such a fitting gave us a fibre volume content of 25%, which is quite low for an unidirectional composite. However, its associated strength is quite low as well (173 MPa) but agrees with such a fibre volume content based on data in [9].

$$E_1 = E_f . V_f + E_m . (1 - V_f) \qquad \text{Eq.2}$$

Table 4: Results from longitudinal tensile tests *values taken from [11] **fitted value

Material	E_1 (GPa)	σ_1 (GPa)	ν_{12}	E_1 based on law of mixture (GPa)
C/PA6*	105.6	1808	0.36	106.8
G/PP	31.1 ± 0.3	531 ± 49	0.27 ± 0.06	34.2
F/Elium	14.4 ± 1.1 10.8 ± 0.4	173 ± 10	0.20 ± 0.08	14.5**
C/GR33	126.7 ± 2.6	1431 ± 31	0.31 ± 0.05	133.2

Table 5: Data from literature used for rule of mixtures calculations

Material	E_{fibres} (GPa)	E_{matrix} (GPa)	V_f (%)	References
C/PA6	220	2.3	48	[10-12]
G/PP	72	0.5	46	[13-14]
F/Elium	50	2.5	25*	[9], [15]
C/GR33	220	3.2	60	[10], [16]

7.1.2 Tests on unidirectional specimens in the transverse direction [90]

Tensile tests were then performed on unidirectional specimens in the transverse direction in order to obtain the transverse modulus E_2 and the transverse strength σ_2. Results are summarized in Table 6 and Stress-strain plots are shown in the Appendix. The three thermoplastic materials all display relatively low transverse strengths ($\sigma_2 \leq 25$ MPa) compared with the C/GR33 material (σ_2>30 MPa). Also, for the G/PP and F/El, the stress strain plots do not show purely elastic behaviour, so transverse strengths were taken as those at the end of linearity, for design purposes.

Table 6: Results from transverse tensile tests *values taken from [11] **values taken at the end of linearity

Material	E_2 (GPa)	σ_2 (MPa)
C/PA6*	5.8	25
G/PP	4.1 ± 2.1	11 ± 1**
F/Elium	3.3 ± 0.2	17 ± 2**
C/GR33	8.2 ± 0.3	33 ± 4

7.1.3 Tests on biaxial specimens [±45] – Shear behaviour

Tensile tests were then performed on ±45° specimens to characterize the shear behaviour (shear modulus G_{12} and shear strength τ_{12}). Results are summarized in Table 7 and plots are found in the Appendix.

Table 7: Results from shear tensile tests *Values taken from [11] **Failures located within the tabs

Material	G_{12} (GPa)	τ_{12} (MPa)
C/PA6*	2.4	37
G/PP	1.6 ± 0.2	18 ± 4**
F/Elium	1.1 ± 0.2	24 ± 1
C/GR33	3.0 ± 0.2	57 ± 1

7.1.4 Data for alternative materials for blade design in the unaged state

Finally, Table 8 summarizes all the results concerning alternative materials for blade design. It may be highlighted that in all cases, scatter is quite low so all these data can be used for blade design with good confidence. Also, the mechanical properties of G/PP and F/Elium™ are quite comparison with C/PA6 and C/GR33.

Table 8: Blade design data on alternative materials in the unaged state

Material	C/PA6	G/PP	Flax/Elium	C/GR33
Condition	Unaged	Unaged	Unaged	Unaged
E_1 (GPa)	105.6	31.1 ± 0.3	14.4 ± 1.1* 10.8 ± 0.4**	126.7 ± 2.6
E_2 (GPa)	5.8	4.1 ± 2.1	3.3 ± 0.2	8.2 ± 0.3
G_{12} (GPa)	2.4	1.6 ± 0.2	1.1 ± 0.2	3.0 ± 0.2
ν_{12}	0.36	0.27 ± 0.06	0.20 ± 0.08	0.31 ± 0.05
σ_1 (MPa)	1808	531 ± 49	173 ± 10	1431 ± 31
σ_2 (MPa)	25	17 ± 1	22 ± 2	33 ± 4
τ_{12} (MPa)	37	18 ± 4**	24 ± 1	57 ± 1
τ_{13} (MPa)	/	/	14 ± 1	50 ± 3

7.2 FLEXURAL TESTS

Results from flexural tests performed on all four materials are summarized in Table 9. Stress-displacement plots are presented in the appendix.

Table 9: Results from flexural tests on [0/90] specimens

Material	$\sigma_{flexure}$ (MPa)
C/PA6	799 ± 31
G/PP	306 ± 3
F/Elium	118 ± 8
C/GR33	463 ± 23

Significant differences in strength are observed between the four materials. More especially, it is quite surprising that the C/GR33 materials fails at a flexural stress below 500 MPa.

8 FLEXURAL FATIGUE BEHAVIOUR

This section is devoted to the flexural fatigue properties of the four alternative materials. All materials have similar stacking sequences $[0/90]_s$. Tests were performed using stress levels between 50 to 90% of the static strength. Results are shown in Figure 11.

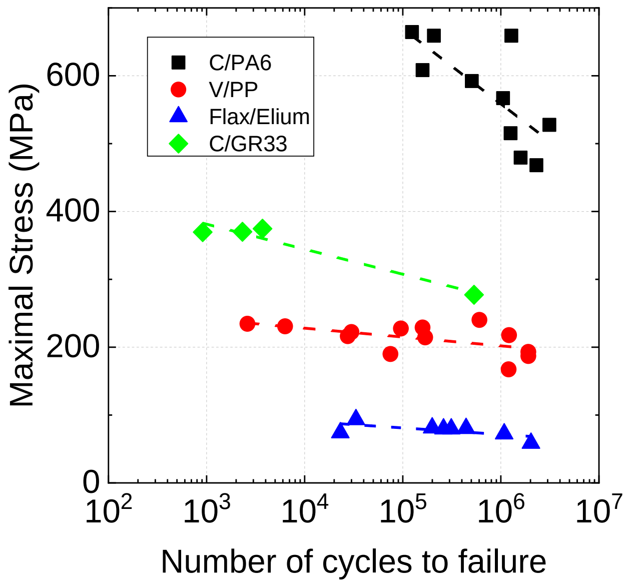

Figure 11: Flexural fatigue strength of alternative materials

Results show that the carbon based materials possess higher flexural strengths, which is in accordance with static flexural tests. Again, it is surprising to see that the C/GR33 material is quite close to the G/PP fatigue curve. This may be associated with the unidirectional fabric used for this material which makes it highly sensitive to micro buckling. Then, if we normalize the results using each material's flexural static strength, results show that the fatigue response curves are fairly similar, Figure 12. The loss in fatigue strength is around 10% per decade.

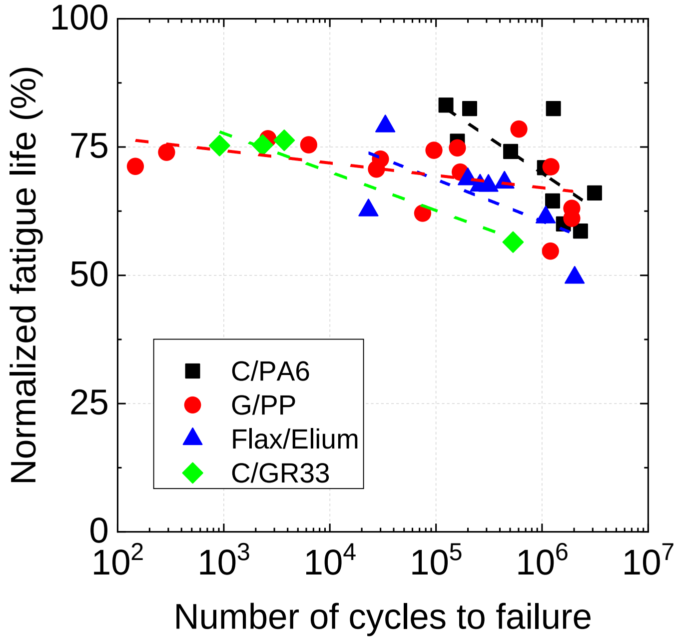

Figure 12: Flexural fatigue results normalized by flexural static strength

9 INFLUENCE OF SEAWATER IMMERSION

This section is now focused on the effect of sea water immersion on the mechanical properties of the C/PA6, G/PP and F/El panels, first under static loading and then in fatigue. Tests were all performed once water saturation was reached, based on the plots in Figure 10.

9.1 QUASI-STATIC PROPERTIES

Here, tests were performed in tension on unidirectionals (longitudinal and transverse) and biaxial (shear) specimens, and in flexure on [0/90] specimens. Results are compiled in Table 10 and Table 11. The G/PP material appears quite unaffected by sea water aging under tensile loading. This may be associated with the fact that both glass fibres and matrix are quite hydrophobic. However, the flexural properties are slightly affected, which may suggest a degradation of the interface between the plies upon aging. Concerning the C/PA6, only the matrix dominated properties appear to be sensitive to sea water aging. Indeed, carbon fibres are insensitive to moisture while the polyamide 6 matrix behavior is known to be quite sensitive to water ingress [12]. On the other hand, all properties of the F/El material are lowered by sea water aging. This is due to the fact that both fibres and matrix are affected by water ingress. It should be noted that all the data presented here can be used for blade design, so as to quantify the effect of aging on the design (both on cost and weight for an equivalent stiffness).

Table 10: Tensile quasi static properties after sea water aging *From [11]

Material	C/PA6*	C/PA6*	G/PP	G/PP	Flax/Elium	Flax/Elium
Condition	Unaged	Saturated	Unaged	Saturated	Unaged	Saturated
E_1 (GPa)	105.6	111	31.1 ± 0.3	36.3 ± 0.9	14.4 ± 1.1	5.2 ± 0.2
E_2 (GPa)	5.8	3.5	4.1 ± 2.1	4.4 ± 1.1	3.3 ± 0.2	1.4 ± 0.3
G_{12} (GPa)	2.4	1.2	1.6 ± 0.2	1.6 ± 0.2	1.1 ± 0.2	0.5 ± 0.1
ν_{12}	0.36	0.42	0.27 ± 0.06	0.37 ± 0.02	0.20 ± 0.08	0.24 ± 0.07
σ_1 (MPa)	1808	/	531 ± 49	551 ± 17	173 ± 10	153 ± 8
σ_2 (MPa)	25	17	17 ± 1	17 ± 1	22 ± 2	17 ± 1
τ_{12} (MPa)	37	21	18 ± 4**	18 ± 4	24 ± 1	16 ± 1
τ_{13} (MPa)	/	/	/	/	14 ± 1	/

Table 11: Static flexural properties after sea water aging

Material	$\sigma_{flexure}$ (MPa)	
	Unaged	Saturated
C/PA6	799 ± 31	380 ± 20
G/PP	306 ± 3	260 ± 8
F/Elium	118 ± 8	78 ± 10

9.2 FATIGUE PROPERTIES

The fatigue behaviour after sea water aging was then investigated under flexure for the three materials. Results are presented in Figure 13 and are compared to those in the unaged state, presented earlier in Figure 11.

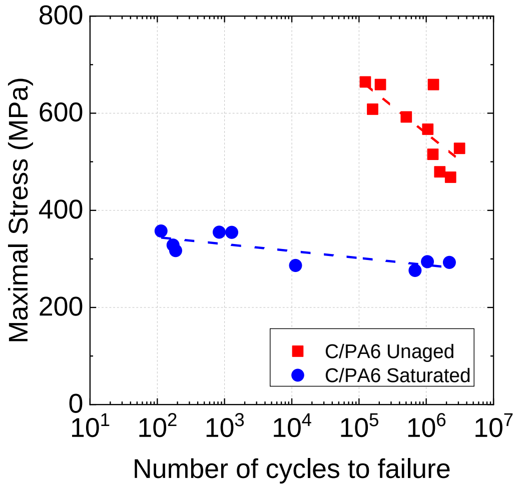

(a)

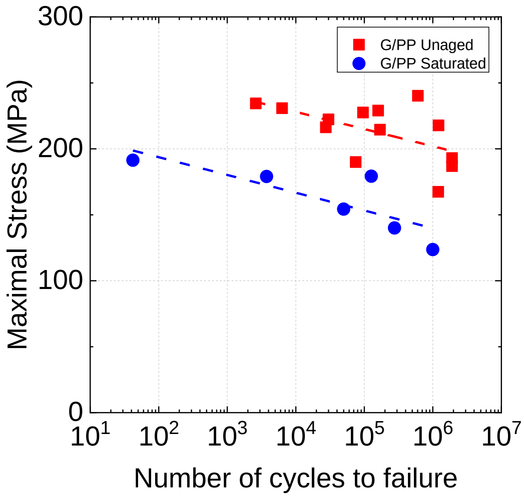

(b)

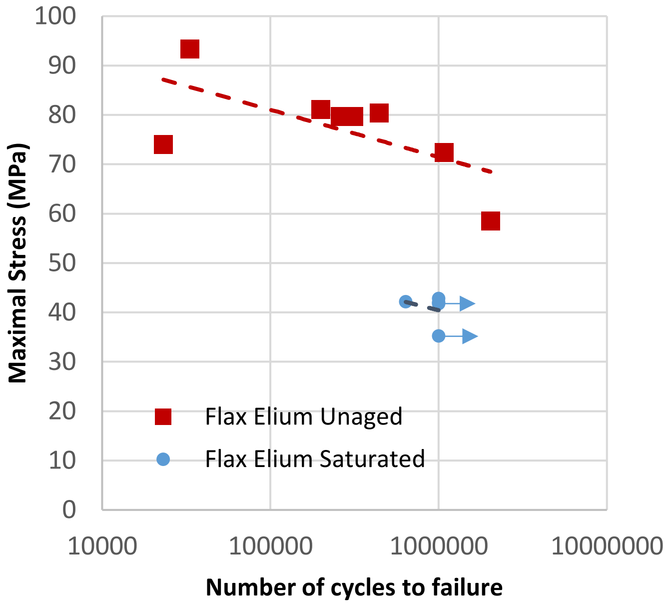

(c)

Figure 13: Effect of sea water aging on the flexural fatigue properties of (a) Carbon/Polyamide 6 (b) Glass/Polypropylene (c) Flax/Elium

In all cases, a significant drop in fatigue behaviour is observed, which is in accordance with static results. Indeed, interface and matrix dominated properties were all affected by sea water aging under static loading. These are directly linked with fatigue resistance.

10 COMPARISON WITH EXISTING EPOXY MATRIX COMPOSITES

As stated in the introduction, the aim of this task is to investigate to what extent materials with reduced environmental impact can be employed as alternatives to fibre reinforced petrochemical based resins in tidal turbines. The four alternative materials presented in the previous sections are now compared to those studied in task 1.3 (carbon and glass/epoxy), which are considered as reference materials for such applications. Because carbon and glass-based composites cannot be directly compared due to their very different stiffnesses, we differentiated the carbon-based materials (Carbon/Epoxy, Carbon/PA6 and Carbon/Greenpoxy33) and the glass-based materials (Glass/epoxy, glass/PP and Flax/Elium). Flax based composites are indeed usually suggested as an alternative for glass-based materials rather than carbon, as their fibre modulus is similar to that of glass fibres.

10.1 QUASI-STATIC PROPERTIES

Results comparing the alternative materials with their associated counterpart from T1.3 are presented in Figure 14. Concerning the carbon-based materials, the data from C/PA6 and C/GR33 are normalized by their associated property from the C/epoxy materials from T1.3. The same goes for the G/PP and F/El materials which are normalized by their associated property from the glass/Epoxy materials from T1.3. For example, Eq.3 shows how the normalized E1 value was calculated in Figure 14. The data for blade design for the carbon and glass/epoxy materials in the unaged state are shown in Table 12.

$$Normalized\ E_1 = \frac{E_{1\ C/PA6}}{E_{1\ C/Epoxy}} \times 100 \qquad \text{Eq.3}$$

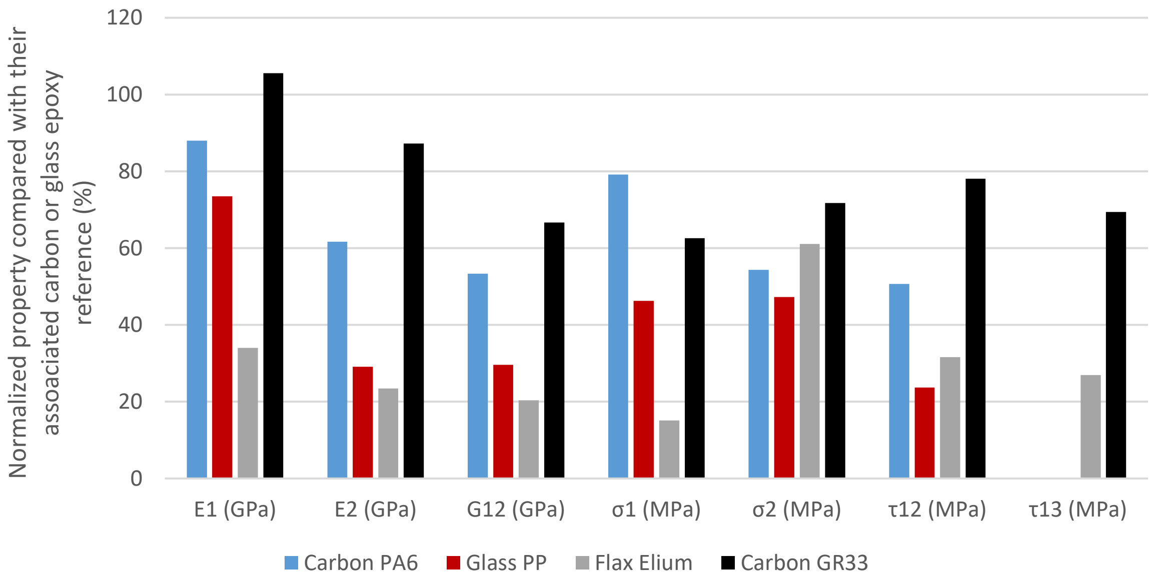

Figure 14: Properties of alternative materials normalized with respect to their carbon and glass epoxy references from T1.3

Table 12: Mechanical properties of carbon and glass epoxy composites from T1.3 for blade design in the unaged state

Material	C/Epoxy	G/Epoxy
E_1 (GPa)	120.3 ± 2.1	42.3 ± 3.6
E_2 (GPa)	9.4 ± 0.3	14.1 ± 0.3
G_{12} (GPa)	4.5 ± 0.4	5.4 ± 0.3
ν_{12}	0.26 ± 0.02	0.34 ± 0.03
σ_1 (MPa)	2285 ± 102	1148 ± 43
σ_2 (MPa)	46 ± 2	36 ± 4
τ_{12} (MPa)	73 ± 7	76 ± 2
τ_{13} (MPa)	72 ± 2	52 ± 3

From Figure 14, it is clear that none of the alternative materials investigated within T5.2 are directly comparable with the carbon and glass/epoxy materials from T1.3. However, the best candidates to replace the reference materials appear to be the C/GR33 (all properties above 60% of the associated reference property) and the C/PA6 (all above 50%). The glass/PP and F/El appear to be further away from their glass/epoxy reference. However, in design, all these materials can be used efficiently because other aspects than mechanical properties can be presented, such as associated cost, weight, and environmental impact, etc.

10.2 FATIGUE PROPERTIES

The fatigue properties are then compared in Figure 15.a for the carbon-based materials and in Figure 15.b for the glass-based materials. All data were normalized by their associated static strength in flexure.

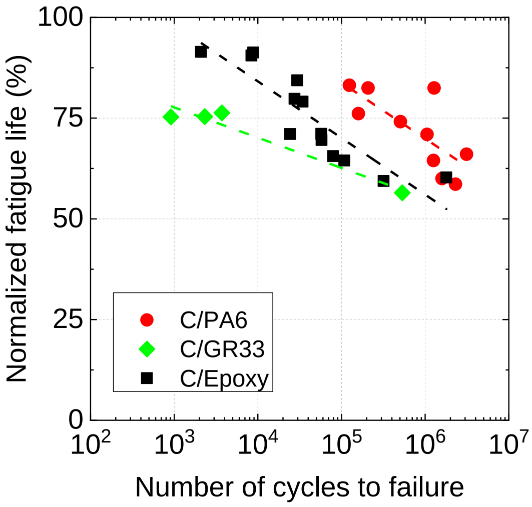

(a)

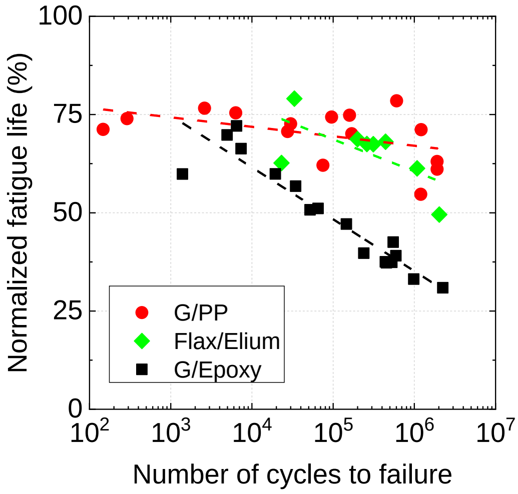

(b)

Figure 15: Normalized fatigue strength by static test values in the unaged state (a) Carbon based materials (b) Glass based materials and F/El material

It is quite interesting to note that all thermoplastic composites investigated within this task (PA6, PP and Elium) have better fatigue resistance than their associated thermoset counterpart when normalized by static strength. Such a result is truly interesting in design.

11 CONCLUSION

This document describes results from a study to examine alternative composite materials for tidal turbine blade manufacture. In total, three thermoplastic composites were examined and a carbon/epoxy material in which the resin is 28% biobased. The mechanical properties in static and in fatigue were characterized on all four materials and the effect of sea water aging was examined. To fully evaluate whether these alternative materials can be used for marine applications, an additional study in which the data is used for blade design is to be performed. Only then can be a conclusion be drawn concerning the potential advantages from these material with respect to the environment.

12 APPENDIX

- Quasi-static properties in the unaged state
    - Longitudinal direction

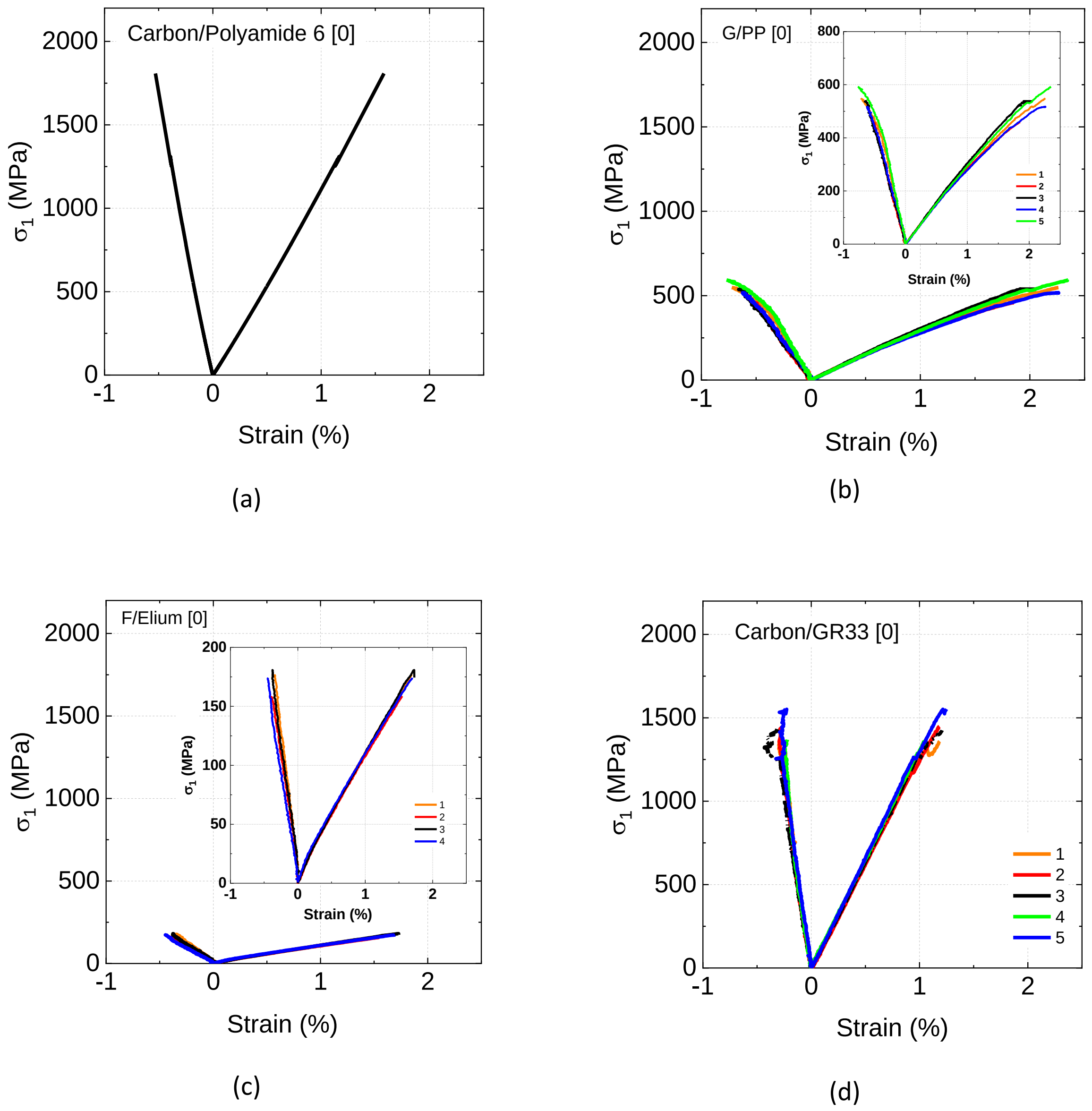

Figure 16: Stress-strain plots from tensile tests in the longitudinal direction (a) Carbon/Polyamide 6 (b) Glass/Polypropylene (c) Flax/Elium (d) Carbon/Greenpoxy 33

- Transverse direction

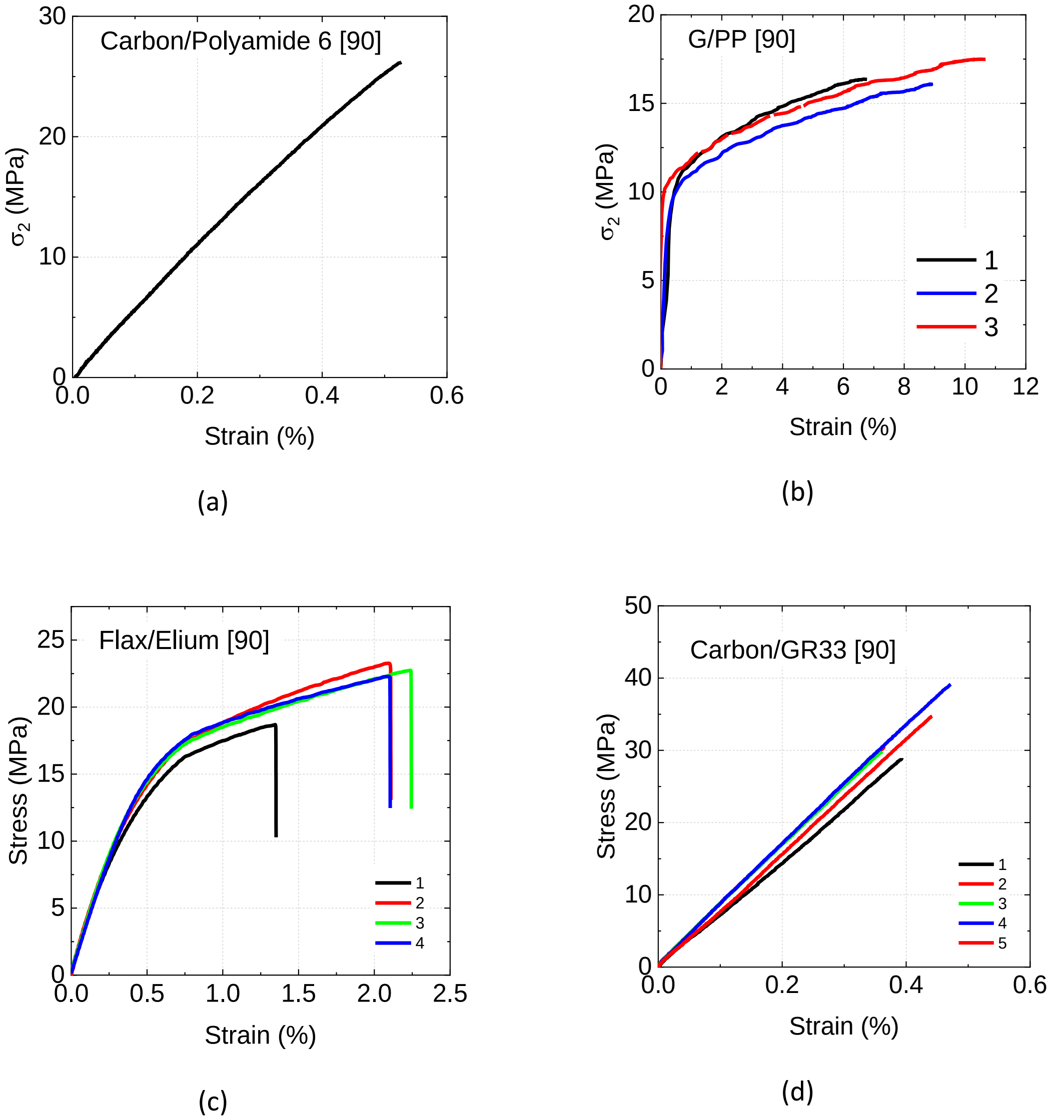

Figure 17: Stress-strain plots from tensile tests in the transverse direction (a) Carbon/Polyamide 6 (b) Glass/Polypropylene (c) Flax/Elium (d) Carbon/Greenpoxy 33

- Shear behaviour

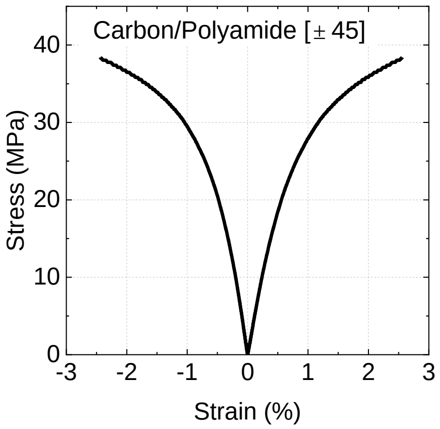

(a)

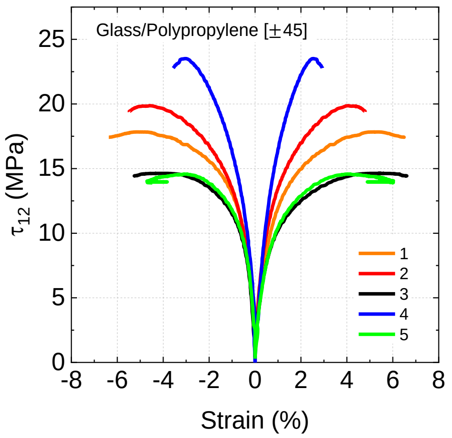

(b)

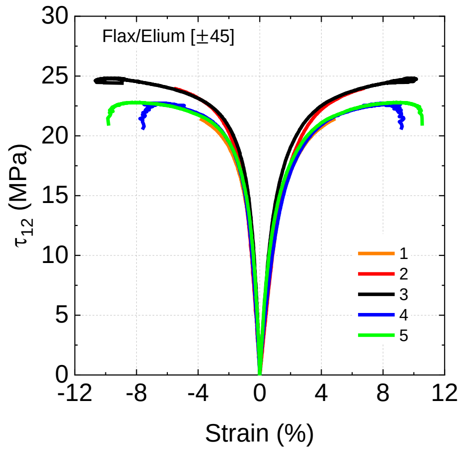

(c)

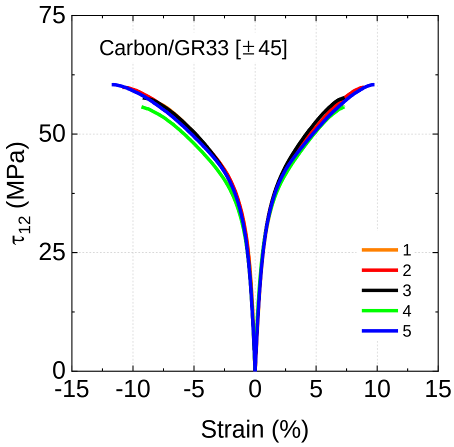

(d)

Figure 18: Stress-strain plots from tensile tests in the shear direction (a) Carbon/Polyamide 6 (b) Glass/Polypropylene (c) Flax/Elium (d) Carbon/Greenpoxy 33

- Flexural tests

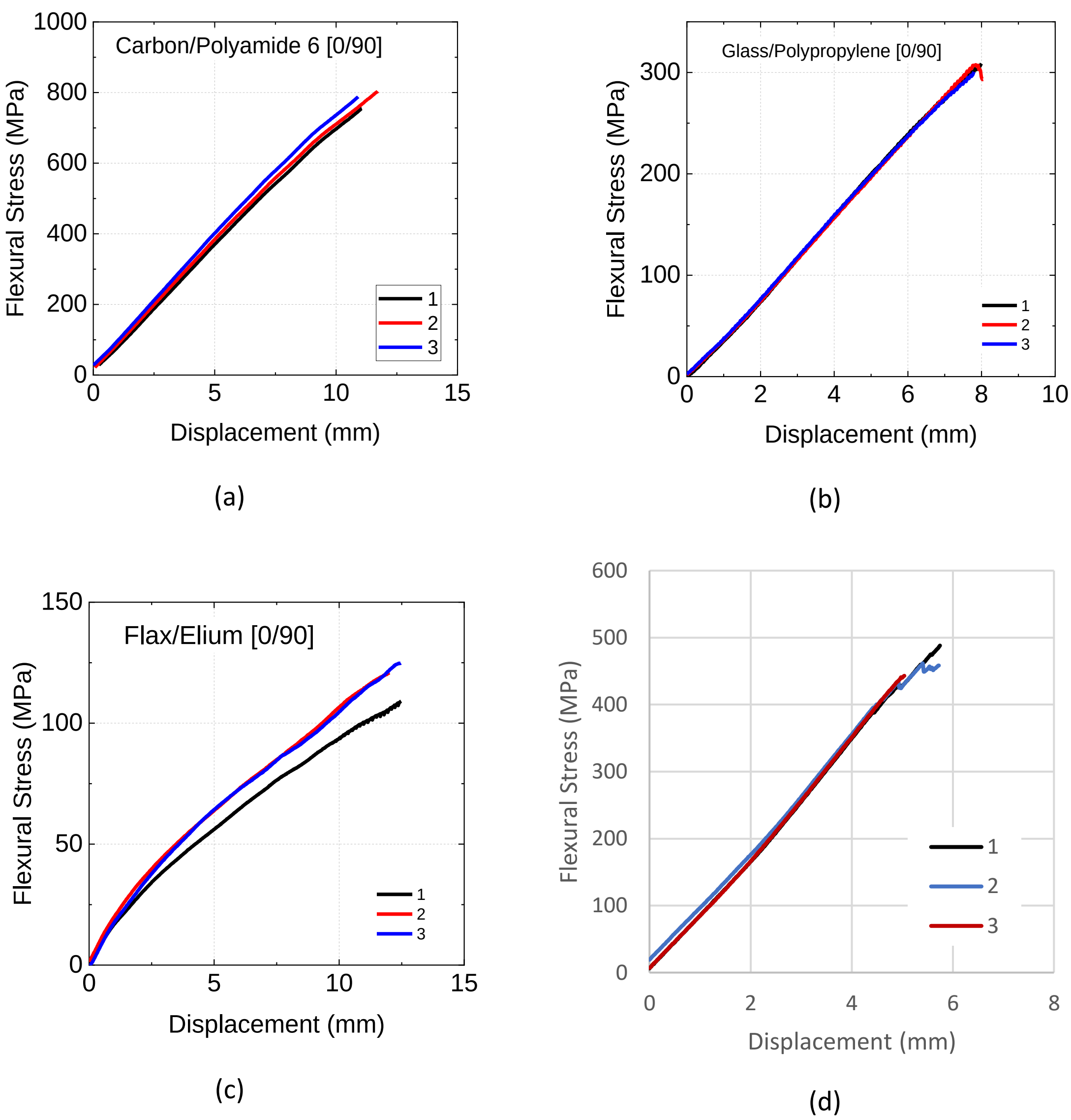

Figure 19: Flexural stress-displacement plots on [0/90] for (a) Carbon/Polyamide 6 (b) Glass/Polypropylene (c) Flax/Elium (d) Carbon/Greenpoxy 33

- Quasi-static properties after sea water aging
  - Longitudinal direction

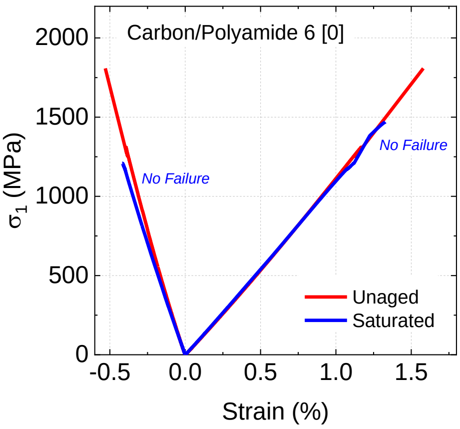

(a)

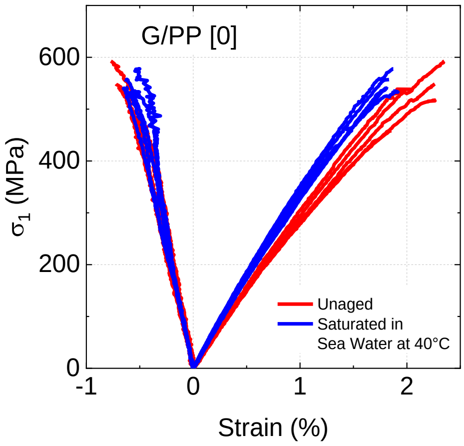

(b)

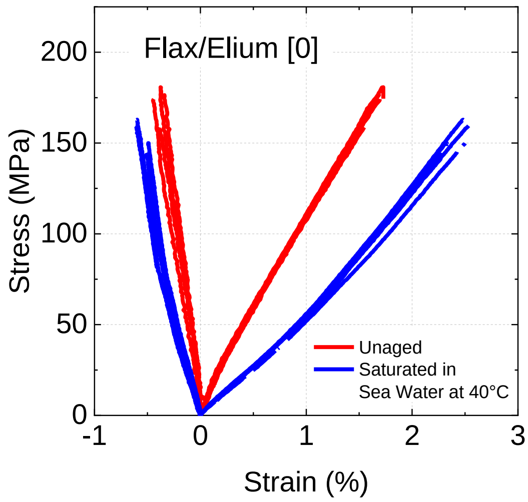

(c)

Figure 20: Effect of sea water aging on the longitudinal properties of (a) Carbon/Polyamide 6 (b) Glass/Polypropylene (c) Flax/Elium

- Transverse direction

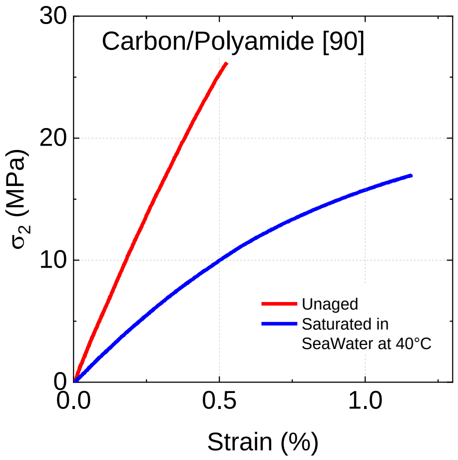

(a)

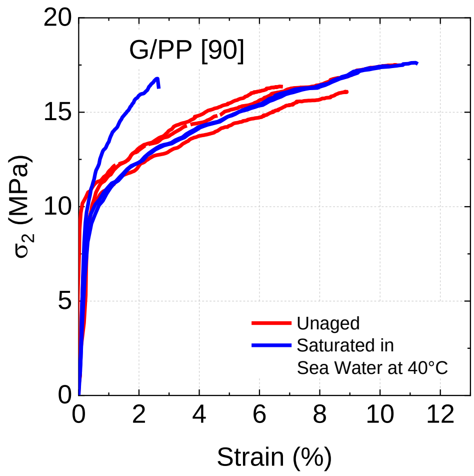

(b)

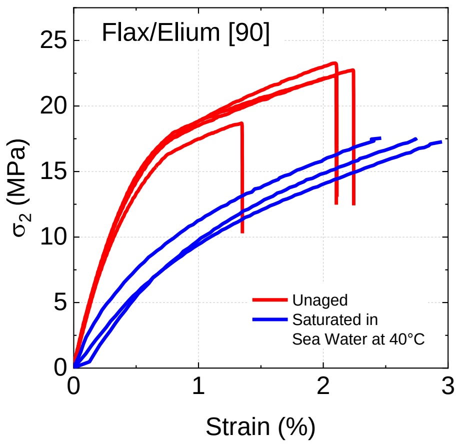

(c)

Figure 21: Effect of sea water aging on the transverse properties of (a) Carbon/Polyamide 6 (b) Glass/Polypropylene (c) Flax/Elium

- Shear behaviour

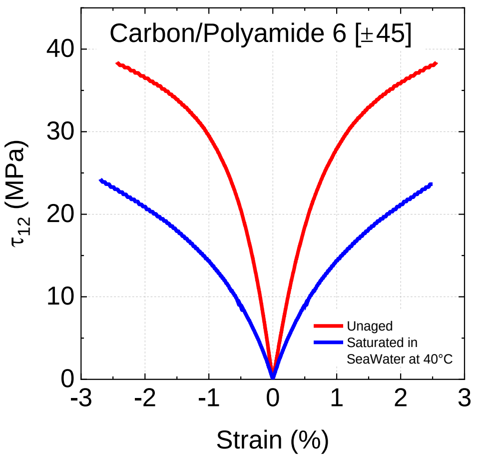

(a)

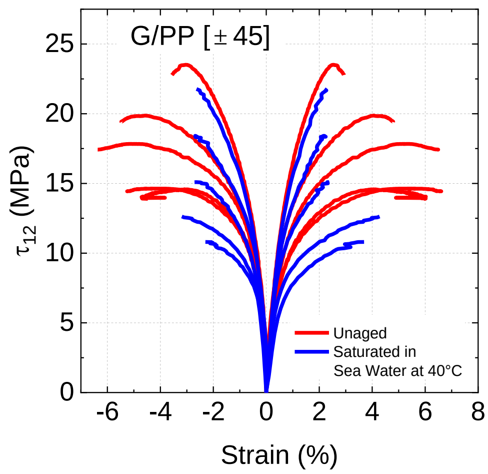

(b)

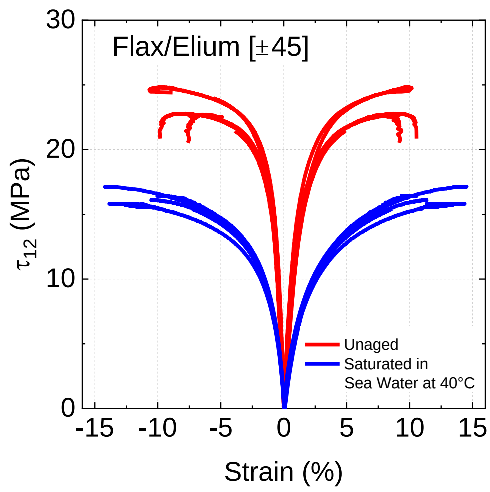

(c)

Figure 22: Effect of sea water aging on the shear properties of (a) Carbon/Polyamide 6 (b) Glass/Polypropylene (c) Flax/Elium

13 REFERENCES

[1] A. Gholampou and T. Ozbakkaloglu, "A review of natural fiber composites: properties, modification and processing techniques, characterization, applications," *Journal of Material Science,* pp. 829-892, 2020.

[2] A. Rekondo and G. Vara, "Novel thermoset composites for more competitive and sustainable industries," *JEC Composites Magazine,* pp. 48-49, October 2020.

[3] H. Lilholt and M. Lawther, "Natural Organic Fibres," in *Comprehensive Materials Volume 1: Fibre reinforcements and General Theory of Composites*, 2000.

[4] K. Pickering, M. A. Efendy and T. Le, "A review of recent developments in natural fibre composites and their mechanical performance," *Composites: Part A,* 2015.

[5] N. H. Bakar, K. M. Hyie, A. S. Ramlan, M. K. Hassan and A. Jumahat, "Mechanical Properties of Kevlar Reinforcement in Kenaf Composites," *Applied Mechanics and Material,* Vols. 465-466, pp. 847-851.

[6] P. N. Khanam, H. P. S. A. Khalil, M. Jawaid, G. R. Reddy, C. S. Narayana and S. V. Naidu, "Sisal/Carbon Fibre Reinforced Hybrid Composites: Tensile, Flexural and Chemical Resistance Properties," *Journal of Polymers and the Environment,* vol. 18, pp. 727-733, 2010.

[7] M. R. Jamir, M. S. Majid and A. Khasri, "Natural lightweight hybrid composites for aircraft structural applications," in *Sustainable Composites for Aerospace Applications*, Elsevier, 2018, pp. 155-170.

[8] J. M. F. A. Blanchard and A. J. Sobey, "Comparative design of E-glass and flax structures based on reliability," *Composite Structures,* 2019.

[9] C. Baley, M. Gomina, J. Breard, A. Bourmaud and P. Davies, "Variability of mechanical properties of flax fibres for composite reinforcement: A review," *Industrial Crops & Products,* 2020.

[10] Kant, M., & Penumadu, D. (2013). Fracture behavior of individual carbon fibers in tension using nano-fabricated notches. *Composites science and technology*, *89*, 83-88.

[11] Arhant, M., Briançon, C., Burtin, C., & Davies, P. (2019). Carbon/polyamide 6 thermoplastic composite cylinders for deep sea applications. *Composite Structures*, *212*, 535-546.

[12] Le Gac, P. Y., Arhant, M., Le Gall, M., & Davies, P. (2017). Yield stress changes induced by water in polyamide 6: characterization and modeling. *Polymer Degradation and Stability*, *137*, 272-280.

[13] Arib, R. M. N., Sapuan, S. M., Ahmad, M. M. H. M., Paridah, M. T., & Zaman, H. K. (2006). Mechanical properties of pineapple leaf fibre reinforced polypropylene composites. *Materials & Design*, *27*(5), 391-396.

[14] Pardini, L. C., & Manhani, L. G. B. (2002). Influence of the testing gage length on the strength, Young's modulus and Weibull modulus of carbon fibres and glass fibres. *Materials research*, *5*(4), 411-420.

[15] Davies, P., Le Gac, P. Y., & Le Gall, M. (2017). Influence of sea water aging on the mechanical behaviour of acrylic matrix composites. *Applied Composite Materials*, *24*(1), 97-111.

[16] Sicomin Epoxy systems (2020) Datasheet SR GreenPoxy 33 SD 477X DNV GL, http://www.sicomin.com/datasheets/product-pdf_fr203.pdf